Detection of the optical counterpart of the transient ULX NGC300 ULX-1: a nascent black hole – neutron star binary?

André-Nicolas Chené [ID],[1] Georgios Vasilopoulos [ID],[2, 3] Lidia M. Oskinova [ID],[4] and Clara Martínez-Vázquez [ID][5]

[1]NSF NOIRLab, 670 N. A'ohoku Place, Hilo, HI, 96720, USA
[2]Department of Physics, National and Kapodistrian University of Athens, University Campus Zografos, GR 15784, Athens, Greece
[3]Institute of Accelerating Systems & Applications, University Campus Zografos, Athens, Greece
[4]Institut für Physik und Astronomie, Universität Potsdam, Karl-Liebknecht-Str. 24/25, 14476 Potsdam, Germany
[5]international Gemini Observatory/NSF NOIRLab, 670 N. A'ohoku Place, Hilo, HI, 96720, USA

ABSTRACT

The end points of massive star evolution are poorly known, especially those in interacting binary systems containing compact objects, such as neutron stars or black holes. Such systems are bright in X-rays, and the most luminous among them are called ultra-luminous X-ray sources (ULXs). In this paper, we address the enigmatic NGC 300 ULX-1. It's X-ray activity started in 2010 with the supernova impostor-like event SN 2010da. In the following few years the ULX was powered by persistent super-Eddington accretion but then it dimmed in X-rays. We present the most recent X-ray and optical observations. The *Chandra* and *Swift* telescopes confirm that SN 2010da/NGC 300 ULX-1 is not accreting at super-Eddington level anymore. We attribute this switch in accretion regime to the donor star variability and its fast evolution. In order to gain a better understanding of the donor star's nature, we consider its optical light curve on a decade-long time scale and show that the optical counterpart of SN 2010da/NGC 300 ULX-1 dimmed significantly over recent years. The most recent detection in optical by the Gemini telescope reveals that the source is now > 2.5 mag fainter in the r' band compared to the epoch when it was spectroscopically classified as a red supergiant. We discuss the nature of the abrupt changes in the donor star properties, and consider among other possibilities the silent collapse of the donor star into a black hole.

1. INTRODUCTION

High-mass X-ray binaries (HMXBs) with X-ray luminosities above $\sim 10^{36}$ erg s^{-1} (in the $0.2 - 60$ keV range) are powered by mass transfer from a massive donor star to a neutron star (NS) or black hole (BH). HMXBs can be persistent, but more commonly, they are transient X-ray sources.

HMXBs with $L_X \gtrsim 10^{39}$ erg s^{-1} are classified as ultra-luminous X-ray sources (ULXs) (see review King et al. 2023). The discovery of ULX pulsars (ULXPs, e.g Bachetti et al. 2014) showed that, at least some ULXs are fueled by super-Eddington accretion onto a NS. However neither the duty cycle of ULXPs nor their evolution and origin are fully understood. Most ULXs/ULXPs exhibit modulation in their X-ray light curves, which is attributed to variability in the outflow that influences the collimation of X-rays along the line of sight (e.g. Gúrpide et al. 2021; Vasilopoulos et al. 2021). Hence, sources may transition between ULX and normal accretion phases, as seen in the recently discovered transient

ULX with an OBe-type donor in the Galaxy (Reig et al. 2020).

Changes in the accretion outflow a onto the NS could be caused by the variability of the donor star. Indeed, most evolved massive stars are variable by nature. A dramatic historic example is the so-called Great Eruption of the Galactic luminous blue variable (LBV) star η Carinae. The star increased optical brightness by ~ 8 mag, ejected a large amount of matter, and subsequently returned to its pre-eruption brightness. In general, the LBV eruptions are energetic enough to be misclassified as supernovae (SNe). This led to the introduction of a new type of transients, the so-called SN impostors (Mauerhan et al. 2013).

One enigmatic SN impostor, SN 2010da, is associated with the transient ULX named NGC 300 ULX-1 (from now on SN 2010da/NGC 300 ULX-1). The intense multiwavelengths observations of SN 2010da/NGC 300 ULX-1 over the last 15 years have revealed its remarkable transformations. The system which was once classified as a persistent ULX where a NS accretes matter from a red superginant (RSG) donor (Heida et al.
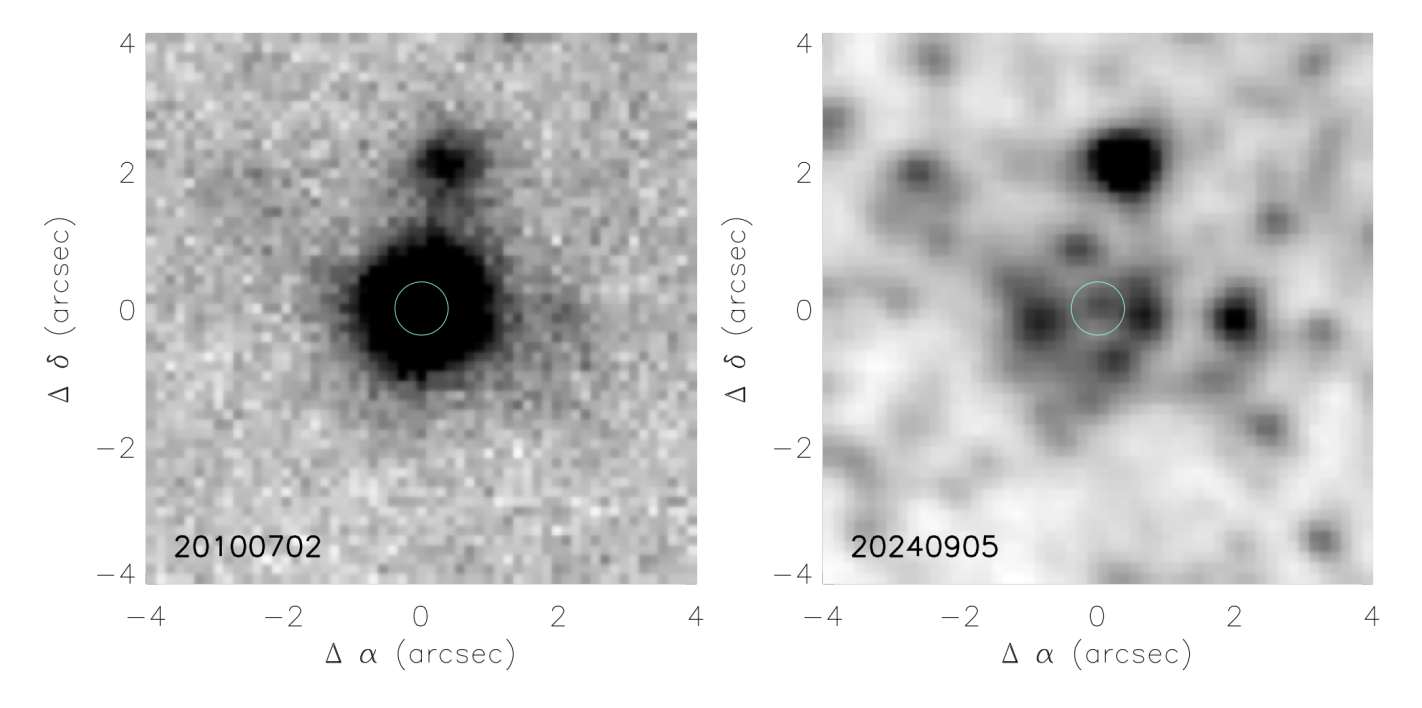
Figure 1. Cut-out from the r'-band GMOS-South images of SN 2010da/NGC 300 ULX-1 taken in 2010 (left) and 2024 (right). The light blue circle marks the position of the source.

2019) is now quiescent. Here, we present the latest X-ray and optical observations of SN 2010da/NGC 300 ULX-1, along with the contemporaneous detection of its optical counterpart.

This paper is organized as follows. In Section 2 we present new r'-band and X-ray monitoring observations as well as the details about constructing long term light-curves in r'-band and X-rays. Section 3 outlines the chronology of events and summarizes observations in X-ray and optical. Sections 4 and 5 present our discussion and conclusions.

2. OBSERVATIONS

2.1. *Optical imaging*

In September 2024, we obtained imaging observations of SN 2010da/NGC 300 ULX-1 using the Gemini South telescope under the program GS-2024B-FT-104. A total exposure time of 2400s was achieved with the GMOS-South instrument (Hook et al. 2004) in imaging mode, using the r' Sloan filter and the new Hamamatsu CCDs (Gimeno et al. 2016). The data were processed and combined using the DRAGONS software package (Labrie et al. 2023). The section of the image around SN 2010da/NGC 300 ULX-1 is shown in the right panel of Figure 1.

Since 2010, the sky field around SN 2010da/NGC 300 ULX-1 has been observed multiple times with different telescopes and instruments, providing valuable archival data for our analysis. Observations in the r' filter with

GMOS-South on the Gemini Observatory are available through the Gemini Observatory Archive. These include a 60-second exposure from July 2010 (program GS-2010-Q-19; left panel of Figure 1) and additional acquisition images taken incidentally during observations of nearby sources. While these acquisition images often have increased noise, shorter exposure times, and suboptimal calibration due to fast readout modes and unstable optics, they remain useful for constructing a historical light curve.

Similarly, an acquisition image obtained with the FORS2 instrument on the Very Large Telescope-U1 (program 105.20HJ) in September 2021, using the GG435 filter, contributes to the photometric dataset. Despite the varied origins and quality of these archival images, they collectively provide sufficient accuracy to support our current analysis.

The photometric reduction was performed using DAOPHOT/ALLSTAR (Stetson 1987, 1994) following similar prescriptions as those described in Martínez-Vázquez et al. 2021. The flux calibration was made using the DECam Local Volume Exploration Survey Data Release 2 (DELVE DR2, Drlica-Wagner et al. 2022)[1]. Unfortu-

---

[1] DELVE DR2 data was downloaded from the Astro Data Lab which is part of the Community Science and Data Center (CSDC) at NSF NOIRLab, the national center for ground-based nighttime astronomy in the United States operated by the Association of Universities for Research in Astronomy (AURA) under cooperative agreement with the U.S. National Science Foundation.

Table 1. X-ray count rates in the 0.5-8.0 keV range and r' photometry of SN 2010da/NGC 300 ULX-1 obtained from from CXO and GMOS-South, respectively.

X-Ray - (0.5-8.0 keV)		Optical	
Date	(10^{-3} c/s)	Date	r' (mag)
2008 Jul 08	<0.4	2010 Jul 02	18.96±0.11
2010 Sep 24	1.20±0.14	2013 Aug 26	20.24±0.17
2014 May 16	0.09±0.04	2017 Jun 19	20.16±0.29
2014 Nov 17	2.21±0.19	2017 Jul 02	20.11±0.13
2018 Feb 08	225±5	2017 Jul 18	20.00±0.17
2018 Feb 11	210±5	2021 Sep 01	<22[†]
2020 Apr 26	0.45±0.10	2024 Sep 05	22.85±0.06

[†]: upper limit evaluated from the photometry of the FORS2 image, converted from the $GG435$ to the r' filter.

nately, the FORS2 acquisition image could not provide better than an upper limit due to low signal. The resulting light curve is presented in Figure 2 and 3, and the extracted values are available in Table 1.

2.2. *X-ray observations*

Following the discovery of X-ray pulsations in 2018, SN 2010da/NGC 300 ULX-1 was extensively monitored by *Swift*/XRT (0.2–10 keV) and *NICER* (0.2–12 keV) X-ray telescopes (see Vasilopoulos et al. 2018; Ray et al. 2019) (see Figure 2). Around August 2018 the X-ray flux dropped, and after some fluctuation the system entered a low flux state (Vasilopoulos et al. 2019). Since that time we have continued monitoring SN 2010da/NGC 300 ULX-1 with *Swift*/XRT aiming at detecting a possible rebrightening. We note that *NICER* observations are only useful during the brightest stage of the system and even then are contaminated by nearby system NGC 300 X-1 (Ng et al. 2022). The field of sky around SN 2010da/NGC 300 ULX-1 has also been observed with *NuSTAR* (3–79 keV), *Chandra* (0.2–12 keV) and *XMM-Newton* (0.2–12 keV) X-ray telescopes. However, among these observatories only *Chandra* allowed meaningful detections at low flux, significantly below the lower limits of *Swift*/XRT individual snapshots. Hence, to gain insights on the behavior of SN 2010da/NGC 300 ULX-1 over time scale of a decade, we construct the X-ray light curve using *Swift*/XRT and *Chandra* data (Figures. 2 and 3).

Archival data were analyzed using `CIAO v4.16` via `conda` with `CALDB v4.11.0`. We constructed clean images in the 0.5-8.0 keV band and performed source detection via `wavdetect`. The latest *Chandra* pointing was performed on April 26 2020 (obsid: 22375, PI: B. Binder), where the source was detected with a rate of

$4.4(1.0)\times10^{-4}$ c/s. The *Swift*/XRT data of sky filed around SN 2010da/NGC 300 ULX-1 were analyzed and a long term X-ray light curve was produced using standard procedures (Evans et al. 2007, 2009). The *Swift*/XRT monitoring of SN 2010da/NGC 300 ULX-1 over 2019-2024 (PI: Vasilopoulos, G.) has a typical cadence of one or two months. During this period, the source is not detected and upper limits could be established. In 2024, a few quite deep observations of the NGC 300 galaxy included the sky field around SN 2010da/NGC 300 ULX-1. These data were stacked in order to obtain an image with a combined exposure time 65 ks. We run source detection on the stacked image and obtained only upper limits for the location of the SN 2010da/NGC 300 ULX-1 with a rate of 0.0004 counts s^{-1}, which is a factor of 10-100 lower compared to the upper limits obtained by the individual XRT snapshots. In order to compute the light-curve we follow the procedure described in Vasilopoulos et al. (2019) and use liner scaling relations to determine the upper limit on $L_{\rm X}$ (0.3-30 keV) assuming the same spectral model as in Carpano et al. (2018). The conversion of the count rate, presented in Table 1, to flux was done using the factors 2.1×10^{40} erg s^{-1}/cnt s^{-1} and 5.6×10^{40} erg s^{-1}/cnt s^{-1} for *Chandra* and XRT, respectively.

To better show the short term evolution of the X-ray light curve we plot individual epochs of interest in Figure 2, while the complete light-curve is presented in Figure 3. In all plots, the time zero is scaled such zero is at the time of the SN 2010da outburst.

We present here an updated light curve characterizing the evolution of the X-ray luminosity of SN 2010da/ NGC 300 ULX-1 following 2018. This marks the period after the last detection of X-ray pulsations from the source

3. FROM OUTBURST TO AFTERMATH

To place the new observations in the context of the longer term evolution, in this section we briefly recap the chronology of events starting shortly before the SN impostor SN 2010da event (see in depth reviews in Villar et al. 2016; Binder et al. 2020). For clarity, we divide these in four phases as illustrated in Figure 3.

3.1. *Phase I. 2010 – 2014*

Before 2010, no source had been detected at the position of SN 2010da/NGC 300 ULX-1 at wavelengths from X-rays (upper limit of $< 10^{37}$ erg s^{-1}, Binder et al. 2011) to optical (conservative limits of 24 AB mag, Berger & Chornock 2010). However, in 2007, the *Spitzer* telescope detected a mid-IR source which brightened by ~ 0.5 mag within six months before the 2010 event (Lau et al. 2016).
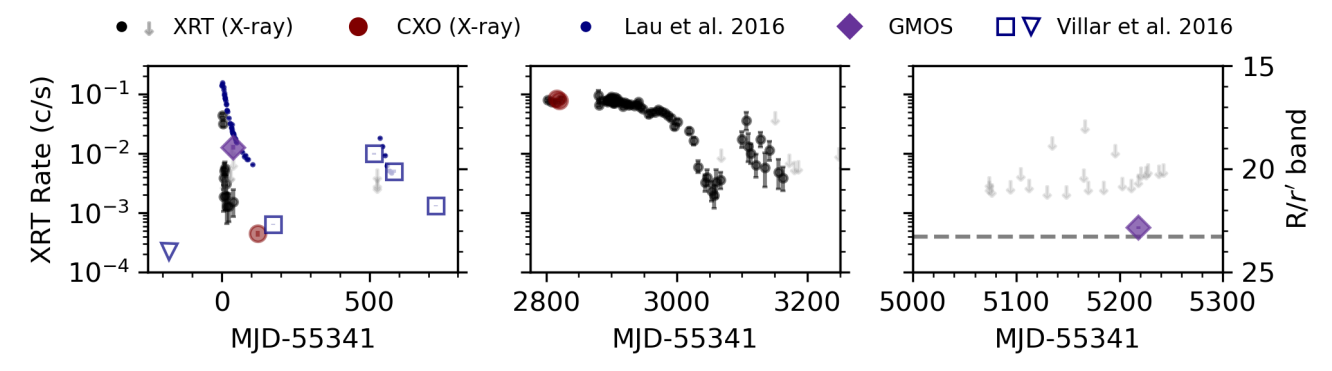
Figure 2. Optical and X-ray light curve zoomed in over 3 epochs. *Left panel:* the SN 2010da event. *Middle panel:* the 2018 campaign that followed the discovery of pulsations and characterization of the system as a ULXP (middle panel). *Right panel:* *Swift*/XRT pointing over 2024. *Swift*/XRT 3σ upper limits are marked with downward gray arrow (values correspond to mid point of arrows). Horizontal hashed line marks upper limit from stacked observations of the 2024 monitoring data.
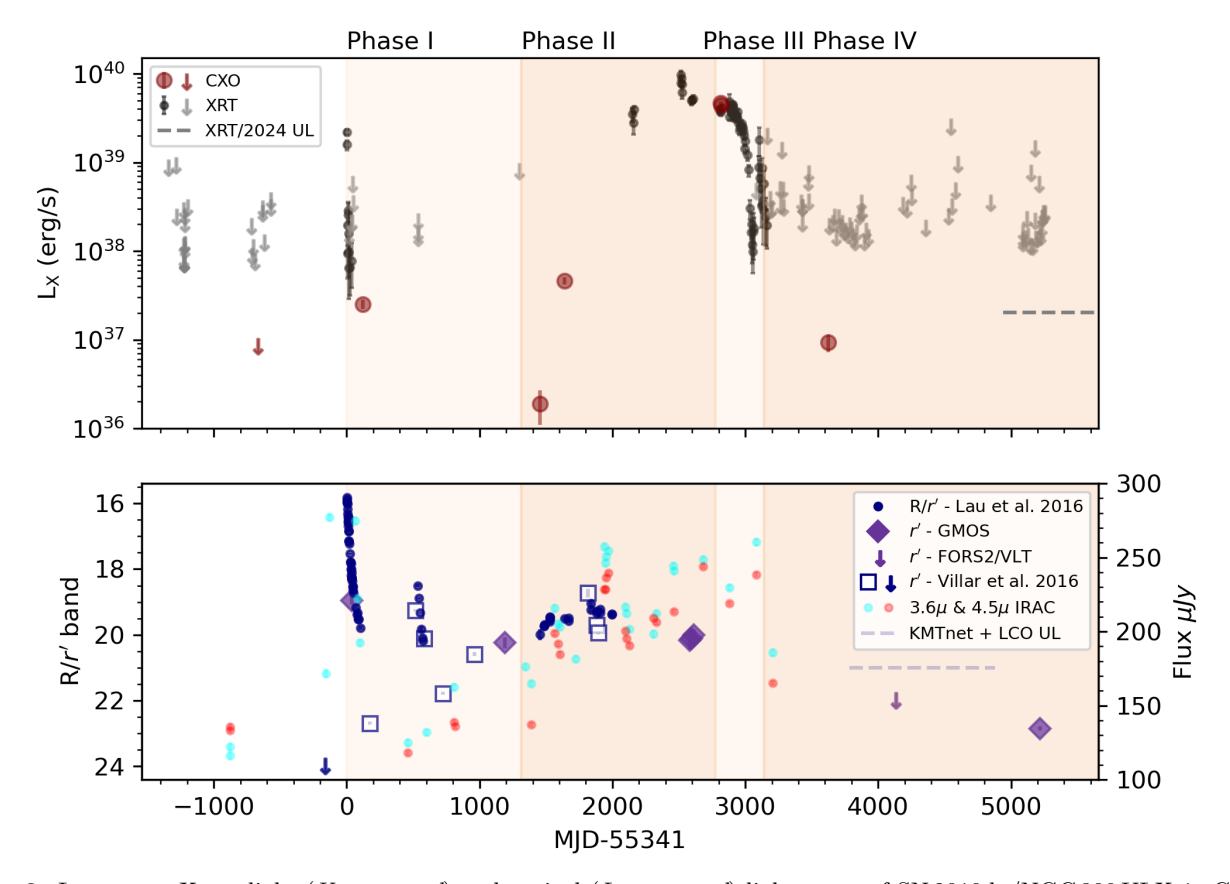

Figure 3. Long term X-ray light (*Upper panel*) and optical (*Lower panel*) light curve of SN 2010da/NGC 300 ULX-1. Characteristic phases following the 2010 impostor event are marked with shaded regions based on X-ray behavior. The L_X is inferred from the count rates assuming constant bolometric correction, i.e. not accounting for changes in absorption. Following the impostor event the X-ray flux drops, while in phase II the flux increases and the source breaks the ULX limit before the flux starts to gradually drop within 2018 (phase III). Within phases II and III there are strong indications that changes in intensity are mainly due to absorption (see text). Within phase IV the source is only detected with deep X-ray observations, and only upper limits were obtained by XRT snapshots or stacked observations. Optical magnitudes are taken from the literature (see text), apart from GMOS which we analyzed. The dashed line shows an upper limit determined by the MKTnet and LCO archival data.

On May 25, 2010, an optical transient, appeared at $r' \approx 16$ mag. Although initially classified as a SN, getting the name SN 2010da, its energetics were much lower than typical for such events. Inspection of the *Spitzer* data shows that the mid-IR flux had raised just before the optical outburst and sharply dropped soon afterward. The X-ray luminosity raised to 5×10^{38} erg s^{-1} at the time of the outburst, but has declined by a factor of 25 within months after (Binder et al. 2011).

3.2. *Phase II. 2014 – 2018*

During 2014 the system remained X-ray active, though at lower levels. But by 2016, *NuSTAR* and *XMM-Newton* observations established that the source became an ULX with the X-ray luminosity $\approx 5 \times 10^{39}$ erg s^{-1}. X-ray pulsations were detected and a spin-up rate of -5.56×10^{-7} s s^{-1} was established. The NS spin rapidly evolved from ~ 126 s in 2014 to ~ 31.5 s in 2016 and to ~ 16.5 s in November 2018. Temporal analysis did not reveal any evidence for orbital modulations, implying either an unlikely pole-on orbital configuration for the system or a large (> 1 yr) orbital period (Carpano et al. 2018; Vasilopoulos et al. 2018, 2019).

X-ray spectral analysis found signs of ultra-fast outflows and a possible cyclotron resonance feature, suggesting a strongly magnetized NS ($\gtrsim 10^{12}$ G; Walton et al. 2018). Comparison of X-ray spectra from 2010 and 2016 showed similar continua but much lower obscuration in 2016 compared to 2010, shortly after the SN 2010da impostor event (Carpano et al. 2018).

3.3. *Phase III. 2018*

By 2018, the optical counterpart of SN 2010da/ NGC 300 ULX-1 had $r' \leq 20.1$ mag. Heida et al. (2019) obtained its optical and near-IR spectra and classified the source as a RSG. The binary orbital period longer than a year is consistent with the the RSG radius (Ray et al. 2019).

Later in 2018, the X-ray flux starts to strongly decline (by a factor of 50 within a year), while the NS spin-up remained constant. This implied that accretion onto the NS has continued but possibly became strongly obscured (Vasilopoulos et al. 2019). Mid-IR emission also sharply declined, possibly explained by the heating of the dust by X-rays.

3.4. *Phase IV. 2019 – now.*

Starting from 2019, the system has further dimmed in X-ray, IR, and optical. Continuing monitoring with *Swift*/XRT returns only upper limits on X-ray luminosity. The last X-ray detection in 2020 (sect. 2.2) measured luminosity of $L_X \approx 10^{37}$ erg s^{-1}. This suggests

that accretion onto the NS was still ongoing at that time, though no longer in a supercritical regime.

Beside the FORS2 archival image and our new r'-band GMOS-South imaging (sect. 2.1), there are no convincing detections neither in optical or IR since 2019. Archival data from the Korean Microlensing Telescope network (KMTnet) and from the Las Cumbres Observatory (LCO) obtained between 2020 and 2021 show some signal that is compatible to an unresolved detection of the group of sources in the vicinity of SN 2010da/ NGC 300 ULX-1 (as seen in Figure 1). We therefore assume a conservative upper limit of ~ 21 mag during that time. The upper limit is estimated as the minimum brightness SN 2010da/NGC 300 ULX-1 would need to reach in order to result into an increased total brightness of the combined signal coming from all the sources within the point spread function (PSF) of the KMTnet and LCO archival data.

4. DISCUSSION

The fast evolution of SN 2010da/NGC 300 ULX-1 during last decade is likely governed by mechanisms acting on short time scales. The new data reported in this paper help to elucidate the nature of these processes.

4.1. *NS spin period and the 2010 event*

X-ray pulsations were discovered in 2014 with long period of 126 s. This suggests that the NS was formed long before the SN 2010da event because young NS typically have spin periods on the order of only 0.1 s or shorter (Igoshev et al. 2022). An alternative scenario where the primary star did collapse into a NS during the SN 2010da event but was spun down rapidly seems very unlikely. While spin reversal due to steady accretion (Vasilopoulos et al. 2018) can help to explain slow rotation, this scenario challenges standard NS formation models and angular momentum conservation in binaries.

The slow NS spin also implies that the super-Eddington accretion episode that powered the ULX between 2010-2018 took place for the first time in the history of SN 2010da/NGC 300 ULX-1. Indeed, if it had happened repeatedly, the NS would have already spun-up to shorter periods before 2014.

4.2. *Donor star variability*

The evolution of light curves across wavelengths from X-rays to mid-IR is linked to the secondary star's activity. Here, we present three possible scenarios.

4.2.1. *RSG variability scenario*

Following Heida et al. (2019) and assuming the donor star is an RSG, the increase in X-ray luminosity ob-

served in 2014 can be explained by a phase of excessive super-Eddington accretion. This may have been triggered by episodic mass loss or a sudden increase in the donor star's radius. Associated dust formation and destruction, along with resulting changes in extinction, further complicate the observed picture.

Mass-loss episodes are frequently observed in RSGs. For example, the well-studied R [W60] B90, RW Cep, μ Cep, and Betelgeuse exhibit episodic mass loss with typical timescales of 200-400 days (e.g., Munoz-Sanchez et al. 2024).

4.2.2. *Radius expansion*

Sudden radius expansion of the donor star is also a possibility. A relevant scenario was proposed by Gilkis et al. (2019), who considered a case where the optical star in a binary system containing an NS rapidly expands due to core instability near the end of its nuclear evolution. As the NS plunges into the stellar envelope, it begins accreting material at a super-Eddington rate, initiating a transient outburst. Once jets are launched, the donor star may either survive or be disrupted.

A similar scenario could apply to SN 2010da/NGC 300 ULX-1 if the NS in this system is on a highly elliptical orbit due to a kick. After the donor star expands, the next periastron passage may lead to the NS grazing the donor star's envelope, triggering the SN impostor event in 2010. The subsequent periastron passage in 2016 could manifest as an ULX phase, eventually leading to the disruption of the donor star.

However, it seems unlikely that the NS and the donor star, hypothetically a RSG, merged around 2020 to form a Thorne-Żytkow object (TŻO, Thorne & Zytkow 1975), as this does not readily explain the optical dimming. Furthermore, the luminosity of the RSG appears too low for a TŻO (Farmer et al. 2023).

4.2.3. *Direct collapse of the donor star*

We speculate that the 2010 SN impostor-like event was indicative of the donor star becoming unstable, a phenomenon often observed among core-collapse SN progenitors (e.g., Qin et al. 2024). This may have led to a brief period of super-Eddington accretion onto the NS, during which the system was observed as an ULX. Accretion ceased when the donor star collapsed without producing an associated SN (Sukhbold & Adams 2020). Although the "failed SN" resulted in some mass ejection, a fraction of the material likely fell back onto the proto-NS, leading to the formation of a BH. The X-ray source observed by *Chandra* in 2020, along with the optical counterpart, was powered by residual accretion.

In this scenario, the current optical source is analogous to failed SN remnants detected in the M31 and NGC 6946 galaxies (Burdge et al. 2024; De et al. 2024). Notably, NGC 6946-BH1 experienced a luminous optical outburst in 2009 (Adams et al. 2017), followed by the formation of an expanding dusty envelope over subsequent years (Basinger et al. 2021). The galactic V404 Cyg triple system is another candidate where evidence suggests BH formation with minimal kick velocity, possibly resulting from a failed supernova (Burdge et al. 2024).

If confirmed through future optical and X-ray monitoring, SN 2010da/NGC 300 ULX-1 would represent the first known example of a failed supernova leading to the formation of a BH-NS binary.

5. SUMMARY AND CONCLUSION

We report the latest X-ray and optical observations of SN 2010da/NGC 300 ULX-1. The system was last detected in X-rays by the *Chandra* telescope in 2020, with a luminosity of $L_X \sim 10^{37} \, \mathrm{erg \, s^{-1}}$, indicating ongoing accretion onto the NS. However, the low flux prevents meaningful spectral or timing analysis of this data. The on-going monitoring with the *Swift* telescope shows that super-Eddington accretion has ceased.

In 2024, we successfully detected the optical counterpart of SN 2010da/NGC 300 ULX-1 using the Gemini telescope. The source is approximately 2.5 magnitudes fainter in the r'-band compared to the last optical detection prior to 2019.

We propose two possible explanations for the observed phenomenology of SN 2010da/NGC 300 ULX-1. One possibility is the interaction of the NS with the supergiant donor, which may have experienced a change in its mass loss or radius. Alternatively, we speculate that within the past five years, the core of the secondary star may have collapsed without producing a SN, suggesting that SN 2010da/NGC 300 ULX-1 has evolved into a relativistic NS+BH binary.

These scenarios will be tested with future observations. If an X-ray binary with $L_X > 10^{35} \, \mathrm{erg \, s^{-1}}$ (as common for NSs accreting from stellar winds) and a stellar counterpart are detected, it would rule out the NS+BH scenario. If the donor star has survived, it should appear either as a hot (bluish) stripped star undergoing a relaxation process or as a cool, RSG-type object. Conversely, if the spectral energy distribution of the source is not stellar and any persistent accretion is moderate, likely from a residual circumstellar nebula, it would be in favor of the NS+BH scenario.

Facilities: Gemini, VLT, *Swift*, *CXO*

Software: DRAGONS (Labrie et al. 2023),

REFERENCES

Adams, S. M., Kochanek, C. S., Gerke, J. R., Stanek, K. Z., & Dai, X. 2017, MNRAS, 468, 4968, doi: 10.1093/mnras/stx816

Bachetti, M., Harrison, F. A., Walton, D. J., et al. 2014, Nature, 514, 202, doi: 10.1038/nature13791

Basinger, C. M., Kochanek, C. S., Adams, S. M., Dai, X., & Stanek, K. Z. 2021, MNRAS, 508, 1156, doi: 10.1093/mnras/stab2620

Berger, E., & Chornock, R. 2010, The Astronomer's Telegram, 2638, 1

Binder, B., Williams, B. F., Kong, A. K. H., et al. 2011, ApJL, 739, L51, doi: 10.1088/2041-8205/739/2/L51

Binder, B. A., Carpano, S., Heida, M., & Lau, R. 2020, Galaxies, 8, 17, doi: 10.3390/galaxies8010017

Burdge, K. B., El-Badry, K., Kara, E., et al. 2024, arXiv e-prints, arXiv:2404.03719, doi: 10.48550/arXiv.2404.03719

Carpano, S., Haberl, F., Maitra, C., & Vasilopoulos, G. 2018, MNRAS, 476, L45, doi: 10.1093/mnrasl/sly030

De, K., MacLeod, M., Jencson, J. E., et al. 2024, arXiv e-prints, arXiv:2410.14778, doi: 10.48550/arXiv.2410.14778

Drlica-Wagner, A., Ferguson, P. S., Adamów, M., et al. 2022, ApJS, 261, 38, doi: 10.3847/1538-4365/ac78eb

Evans, P. A., Beardmore, A. P., Page, K. L., et al. 2007, A&A, 469, 379, doi: 10.1051/0004-6361:20077530

—. 2009, MNRAS, 397, 1177, doi: 10.1111/j.1365-2966.2009.14913.x

Farmer, R., Renzo, M., Götberg, Y., et al. 2023, MNRAS, 524, 1692, doi: 10.1093/mnras/stad1977

Gilkis, A., Soker, N., & Kashi, A. 2019, MNRAS, 482, 4233, doi: 10.1093/mnras/sty3008

8

Gimeno, G., Roth, K., Chiboucas, K., et al. 2016, in Society of Photo-Optical Instrumentation Engineers (SPIE) Conference Series, Vol. 9908, Ground-based and Airborne Instrumentation for Astronomy VI, ed. C. J. Evans, L. Simard, & H. Takami, 99082S, doi: 10.1117/12.2233883

Gúrpide, A., Godet, O., Vasilopoulos, G., Webb, N. A., & Olive, J. F. 2021, A&A, 654, A10, doi: 10.1051/0004-6361/202140781

Heida, M., Lau, R. M., Davies, B., et al. 2019, ApJL, 883, L34, doi: 10.3847/2041-8213/ab4139

Hook, I. M., Jørgensen, I., Allington-Smith, J. R., et al. 2004, PASP, 116, 425, doi: 10.1086/383624

Igoshev, A. P., Frantsuzova, A., Gourgouliatos, K. N., et al. 2022, MNRAS, 514, 4606, doi: 10.1093/mnras/stac1648

King, A., Lasota, J.-P., & Middleton, M. 2023, NewAR, 96, 101672, doi: 10.1016/j.newar.2022.101672

Labrie, K., Simpson, C., Cardenes, R., et al. 2023, Research Notes of the American Astronomical Society, 7, 214, doi: 10.3847/2515-5172/ad0044

Lau, R. M., Kasliwal, M. M., Bond, H. E., et al. 2016, ApJ, 830, 142, doi: 10.3847/0004-637X/830/2/142

Martínez-Vázquez, C. E., Salinas, R., & Vivas, A. K. 2021, AJ, 161, 120, doi: 10.3847/1538-3881/abd55e

Mauerhan, J. C., Smith, N., Filippenko, A. V., et al. 2013, MNRAS, 430, 1801, doi: 10.1093/mnras/stt009

Munoz-Sanchez, G., de Wit, S., Bonanos, A. Z., et al. 2024, A&A, 690, A99, doi: 10.1051/0004-6361/202450737

Ng, M., Remillard, R. A., Steiner, J. F., Chakrabarty, D., & Pasham, D. R. 2022, ApJ, 940, 138, doi: 10.3847/1538-4357/ac9965

Qin, Y.-J., Zhang, K., Bloom, J., et al. 2024, MNRAS, 534, 271, doi: 10.1093/mnras/stae2012

Ray, P. S., Guillot, S., Ho, W. C. G., et al. 2019, ApJ, 879, 130, doi: 10.3847/1538-4357/ab24d8

Reig, P., Fabregat, J., & Alfonso-Garzón, J. 2020, A&A, 640, A35, doi: 10.1051/0004-6361/202038333

Stetson, P. B. 1987, PASP, 99, 191, doi: 10.1086/131977

—. 1994, PASP, 106, 250, doi: 10.1086/133378

Sukhbold, T., & Adams, S. 2020, MNRAS, 492, 2578, doi: 10.1093/mnras/staa059

Thorne, K. S., & Zytkow, A. N. 1975, ApJL, 199, L19, doi: 10.1086/181839

Vasilopoulos, G., Haberl, F., Carpano, S., & Maitra, C. 2018, A&A, 620, L12, doi: 10.1051/0004-6361/201833442

Vasilopoulos, G., Koliopanos, F., Haberl, F., et al. 2021, ApJ, 909, 50, doi: 10.3847/1538-4357/abda49

Vasilopoulos, G., Petropoulou, M., Koliopanos, F., et al. 2019, MNRAS, 488, 5225, doi: 10.1093/mnras/stz2045

Villar, V. A., Berger, E., Chornock, R., et al. 2016, ApJ, 830, 11, doi: 10.3847/0004-637X/830/1/11

Walton, D. J., Bachetti, M., Fürst, F., et al. 2018, ApJL, 857, L3, doi: 10.3847/2041-8213/aabadc